Gen. Math. Notes, Vol. 33, No. 2, April 2016, pp.40-59
ISSN 2219-7184; Copyright ©ICSRS Publication, 2016
www.i-csrs.org
Available free online at http://www.geman.in

A Fully Implicit Finite Difference Scheme for the Regularized Long Wave Equation

Bilge İnan[1] and Ahmet Refik Bahadır[2]

[1]Department of Mathematics, Muallim Rıfat Faculty of Education
Kilis 7 Aralık University, Kilis, Turkey
E-mail: bilgeinan@kilis.edu.tr
[2]Department of Mathematics, Faculty of Arts and Science, İnönü University
Malatya, Turkey
E-mail: refik.bahadir@inonu.edu.tr

(Received: 21-1-16 / Accepted: 15-4-16)

Abstract

In the present paper a numerical solution of the regularized long wave (RLW) equation with a fully implicit finite difference method is deduced. Numerical results for different particular cases of the problem are presented. Comparisons are made with published numerical and analytical solutions. The accuracy of the numerical solutions showed that the present method is well suited for the solution of the RLW equation.

Keywords: *Regularized long wave equation, Finite differences, Solitary waves, Implicit finite difference method.*

1 Introduction

The non-linear regularized long wave (RLW) equation, derived for long waves propagating with dispersion processes, has the following form,

$$\frac{\partial u}{\partial t} + \frac{\partial u}{\partial x} + \varepsilon u \frac{\partial u}{\partial x} - \mu \frac{\partial}{\partial t}\left(\frac{\partial^2 u}{\partial x^2}\right) = 0 \tag{1}$$

where u is the wave amplitude, μ and ε are positive parameters. Physical boundary conditions require $u \longrightarrow 0$ as $x \longrightarrow \pm\infty$. The equation was first obtained by Peregrine [23].

In the literature, many numerical methods have been proposed and implemented for approximating solution of the RLW equation. Gardner and Gardner defined a scheme for the numerical solution of equation based on Galerkin's method using cubic splines as element shape functions [14] while Gardner et al. presented a least-squares technique using linear space-time finite elements for solving RLW equation [15], Dağ [5] studied the least-squares finite element technique which leads to a Petrov-Galerkin method, in which quadratic B-splines as both shape and weight functions were employed over elements. Dogan [9] has drived a Petrov-Galerkin method using quadratic B-spline finite elements for the numerical solution of Eq. (1). Soliman and Raslan [29] gave a collocation method using quadratic B-splines at the mid points whereas Zaki [30] proposed a splitting technique together with cubic B-splines as the element "shape" and "weight" functions throughout the solution region. Dogan [10] defined Galerkin's method for solving the RLW equation using linear space finite elements. In comparison to Dağ et al. [6] who obtained the numerical solution of the equation by using a splitting up technique and both quadratic and cubic B-splines, Raslan [25] suggested a collocation method using cubic B-spline finite elements at the points. Dağ et al. [7] solved the RLW equation by using the quintic B-spline Galerkin finite element method. A numerical method for solving the regularized long wave equation set up based on a Galerkin method with quadratic B-spline finite elements by Esen and Kutluay [13]. Saka and Dağ [27] studied the collocation method based on quartic B-spline interpolation for solution of the RLW equation on one hand Saka et al. [28] presented both sextic and septic B-spline collocation algorithms for the numerical solutions of the RLW equation on the other hand Elibeck and McGuire developed various finite difference methods for solving the RLW equation [11, 12]. Lin [21] used a numerical method based on cubic splines in tension for solving the equation. Gheorghiu [16] construct a stable spectral collocation method for solving the RLW equation. Jain et al. [18] used the combined approach of quasilinearization and invariant imbedding for computing solution of the nonlinear RLW equation. Bhardwaj and Shankar [4] defined a finite difference scheme based on operator splitting and quintic spline interpolation functions technique. Kutluay and Esen [19] gave a linearized implicit finite difference method to obtain numerical solution of the equation. Several finite difference methods were employed to study the solitary waves of the EW and RLW equations by Ramos [24]. Lin et al. [20] studied the RLW equation by high-order compact difference scheme, based on the fourth-order compact scheme in space and fourth-order Runge-Kutta method in time integration. Dağ et al. [8] applied the differential quadrature method based on cosine expansion. Saka et al. [26] set up a space-splitting technique and quadratic B-spline Galerkin finite element method. Araújo and Durán [1] presented the error propagation of time integrators of solitary wave solutions for the equation by using a geometric interpretation of these waves as relative equilibria.

On the other hand, the fully implicit finite difference schemes are high-accuracy schemes for the numerical solution of the nonlinear problems. Bahadır employed the fully implicit finite difference method to compute an approximation to the solution of 1D [2] and 2D [3] Burgers' equations. Moreover, fully implicit finite difference method used for solving equal width wave equation by Inan and Bahadir [17]

In this paper, we develop a fully implicit finite difference scheme for solving the RLW equation. In here, as different from the previous finite difference methods, fully implicit finite difference method is applied to directly the nonlinear RLW equation. Efficiency and validity of the method tested with several different examples and comparisons with the solutions obtained by other methods.

This paper is organized in four sections. In Section 2, we defined the fully implicit finite difference scheme for the RLW equation. Numerical examples are given in Section 3. Section 4 contains some conclusions.

2 The Method of Solution

The discretization is done by the finite differences with the implicit approach of solutions. Solution domain is discretized into cells defined as the nodes set (x_i, t_n) in which $x_i = ih$, $(i = 0, 1, 2, ..., N)$ and $t_n = nk$, $(n = 0, 1, 2, ...)$, h is the spatial mesh size and k is the time step.

Eq. (1) can be written in the following form:

$$\frac{\partial u}{\partial t} + \frac{\partial u}{\partial x} + \varepsilon \frac{\partial}{\partial x}\frac{u^2}{2} - \mu \frac{\partial}{\partial t}\left(\frac{\partial^2 u}{\partial x^2}\right) = 0 \tag{2}$$

The derivatives in Eq. (2) can be approximated at $x = x_i$ and $t = t_n$, to second order in h and k, by

$$\begin{aligned}
\frac{\partial u}{\partial t} &\cong \frac{U_i^{n+1} - U_i^n}{k} \\
\frac{\partial u}{\partial x} &\cong \frac{1}{2}\left[\frac{U_{i+1}^{n+1} - U_{i-1}^{n+1}}{2h} + \frac{U_{i+1}^{n} - U_{i-1}^{n}}{2h}\right] \\
\frac{\partial}{\partial x}\frac{u^2}{2} &\cong \frac{1}{4}\left[\frac{\left(U_{i+1}^{n+1}\right)^2 - \left(U_{i-1}^{n+1}\right)^2}{2h} + \frac{\left(U_{i+1}^{n}\right)^2 - \left(U_{i-1}^{n}\right)^2}{2h}\right] \\
\frac{\partial}{\partial t}\left(\frac{\partial^2 u}{\partial x^2}\right) &\cong \frac{1}{k}\left[\frac{U_{i+1}^{n+1} - 2U_i^{n+1} + U_{i-1}^{n+1}}{h^2} - \frac{U_{i+1}^{n} - 2U_i^{n} + U_{i-1}^{n}}{h^2}\right].
\end{aligned}$$

Putting these approximations in (2), we get

$$\frac{U_i^{n+1}-U_i^n}{k}+\frac{1}{4h}\left[U_{i+1}^{n+1}-U_{i-1}^{n+1}+U_{i+1}^{n}-U_{i-1}^{n}\right]$$

$$+\frac{\varepsilon}{8h}\left[\left(U_{i+1}^{n+1}\right)^2-\left(U_{i-1}^{n+1}\right)^2+\left(U_{i+1}^{n}\right)^2-\left(U_{i-1}^{n}\right)^2\right]$$

$$-\frac{\mu}{kh^2}\left[U_{i+1}^{n+1}-2U_i^{n+1}+U_{i-1}^{n+1}-U_{i+1}^{n}+2U_i^{n}-U_{i-1}^{n}\right]=0 \tag{3}$$

which is valid for values of i lying in the interval $1 \leq i \leq N-1$ and the truncation error in Eq. (3) is $O(k^2)+O(h^2)$. This means that the present method is a first-order accurate method. Where U_i^n denotes the finite difference approximation at the grid point (x_i, t_n) to the exact solution $u(x,t)$. Since Eq. (3) contains $\left(U_{i+1}^{n+1}\right)^2$ and $\left(U_{i-1}^{n+1}\right)^2$ terms, this scheme is called fully implicit finite difference scheme.

This equation is a system of nonlinear difference equations. Let us consider this nonlinear system of equations in the form

$$\mathbf{F}(\mathbf{V})=\mathbf{0} \tag{4}$$

where $\mathbf{F}=[f_1,f_2,\ldots,f_{N-1}]^T$ and $\mathbf{V}=\left[U_1^{n+1},U_2^{n+1},\ldots,U_{N-1}^{n+1}\right]^T$. Newton's method applied to Eq. (4) results in the following iteration:

1. Set $\mathbf{V}^{(0)}$, an initial guess.
2. For $m=0,1,2,\ldots$ until convergence do:
   Solve $J(\mathbf{V}^{(m)})\mathbf{\Delta}^{(m)}=-F(\mathbf{V}^{(m)})$;

Set $\mathbf{V}^{(m+1)}=\mathbf{V}^{(m)}+\mathbf{\Delta}^{(m)}$ where $J(\mathbf{V}^{(m)})$ is the Jacobian matrix which is evaluated analytically[2]. As the initial estimate taken the solution at the previous time-step. Stopping Criteria for the Newton's iteration at each time-step taken as$\left\|\mathbf{F}(\mathbf{V}^{(m)})\right\|_\infty \leq 10^{-5}$. The convergence of the newton method is generally obtained in two or three iterations.

3 Test Problems and Discussion

In this section, some test problems have been considered to illustrate the performance of the method defined in previous section.

The accuracy of the method is measured by using the error norms L_2 and L_∞ defined by

$$\begin{aligned} L_2 &= \|u-U\|_2 = \left(h\sum_{i=0}^{N}|u_i-U_i|^2\right)^{\frac{1}{2}}, \\ L_\infty &= \|u-U\|_\infty = \max_{0\le i\le N}|u_i-U_i|. \end{aligned} \tag{5}$$

where u and U represent the exact and approximate solutions, respectively. We also examined our results by calculating the following three conserved quantities corresponding to mass, momentum and energy [22], respectively [30].

$$\begin{aligned} I_1 &= \int_{-\infty}^{+\infty} u dx \simeq h\sum_{i=0}^{N}U_i^n, \\ I_2 &= \int_{-\infty}^{+\infty} \left(u^2+\mu\,(u_x)^2\right)dx \simeq h\sum_{i=0}^{N}\left[(U_i^n)^2+\mu\left((U_x)_i^n\right)^2\right], \\ I_3 &= \int_{-\infty}^{+\infty} \left[u^3+3u^2\right]dx \simeq h\sum_{i=0}^{N}\left[(U_i^n)^3+3\,(U_i^n)^2\right]. \end{aligned} \tag{6}$$

To give a clear overview of the methodology, the following examples will be discussed.

3.1 Motion of Single Solitary Wave

We first model the motion of a single solitary wave of the RLW equation. The solitary wave analytical solution of the RLW equation (1) is

$$u(x,t) = 3c\,\mathrm{sech}^2(p(x-vt-x^*)) \tag{7}$$

with amplitude $3c$ where $v = 1+\varepsilon c$ is the wave velocity and $p = (\frac{\varepsilon c}{4\mu v})^{1/2}$ measures width of the wave pulse. The initial and boundary conditions are set to: $u(x,0) = 3c\,\mathrm{sech}^2(p(x-x^*))$ and $u \longrightarrow 0$ as $x \longrightarrow \pm\infty$, respectively.

The analytical values of conservation quantities can be found as [30]

$$I_1 = \frac{6c}{p},\; I_2 = \frac{12c^2}{p}+\frac{48pc^2\mu}{5},\; I_3 = \frac{36c^2}{p}\left(1+\frac{4c}{5}\right). \tag{8}$$

To allow comparison with the previous method parameters are taken as $\mu = 1$ and $\varepsilon = 1$.

The analytical invariants for $c = 0.03$ found using Eq. (8) are $I_1 = 2.109407$, $I_2 = 0.127302$ and $I_3 = 0.388806$. Table 1 displays invariants and error norms for $c = 0.03$, $x^* = 0$, the space step $h = 0.1$ and the time step $k = 0.2$ through the interval $-40 \le x \le 60$. The invariants and error norms of the proposed scheme are given for times up to $t = 20$ in Table 1. Table 2 shows L_2 and L_∞ error norms for different values of h and k at $t = 20$. The numerical solution of single solitary wave for $c = 0.03$ at different time is given in Fig. 1. A comparison of invariants obtained by the present method and the result of references [5, 8, 15, 20, 25] is listed in Table 3 for $c = 0.03$ at $t = 20$.

Table 1: Invariants and error norms for the single solitary wave for$h = 0.1$, $k = 0.2$, $-40 \le x \le 60$ and $c = 0.03$.

t	I_1	I_2	I_3	L_2	L_∞
0	2.107027	0.127303	0.388805		
2	2.107799	0.127303	0.388806	0.000070	0.000074
4	2.108424	0.127303	0.388806	0.000150	0.000123
6	2.108956	0.127303	0.388807	0.000237	0.000152
8	2.109408	0.127303	0.388807	0.000323	0.000166
10	2.109778	0.127303	0.388808	0.000401	0.000174
12	2.110046	0.127303	0.388808	0.000468	0.000179
14	2.110187	0.127303	0.388808	0.000524	0.000182
16	2.110173	0.127303	0.388808	0.000570	0.000184
18	2.109962	0.127303	0.388808	0.000608	0.000186
20	2.109491	0.127303	0.388807	0.000642	0.000233

Table 2: Error norms for the single solitary wave for different values of h, k, $-40 \le x \le 60$ and $c = 0.03$ at $t = 20$.

	$h = 0.2$		$h = 0.1$		$h = 0.05$	
k	L_2	L_∞	L_2	L_∞	L_2	L_∞
0.4	0.000427	0.000113	0.000682	0.000233	0.000949	0.000315
0.2	0.000322	0.000114	0.000642	0.000233	0.000924	0.000315
0.1	0.000304	0.000114	0.000638	0.000233	0.000922	0.000315

Table 3: Comparison of invariants for $-40 \le x \le 60$, $c = 0.03$ at $t = 20$.

Method	I_1	I_2	I_3
Analytical	2.109407	0.127302	0.388806
Present Method ($h = 0.1,\ k = 0.2$)	2.109491	0.127303	0.388807
[5] ($h = 0.125,\ k = 0.1$)	2.10769	0.127260	0.388677
[8] ($h = 3,\ k = 0.1$)	2.10471	0.127588	0.392029
[15] ($h = 0.125,\ k = 0.1$)	2.103622	0.1271840	0.3884398
[20] ($h = k = 0.1$)	2.1067778	0.1273011	0.3888043
[25] ($h = k = 0.1$)	2.10352	0.12730	0.38880

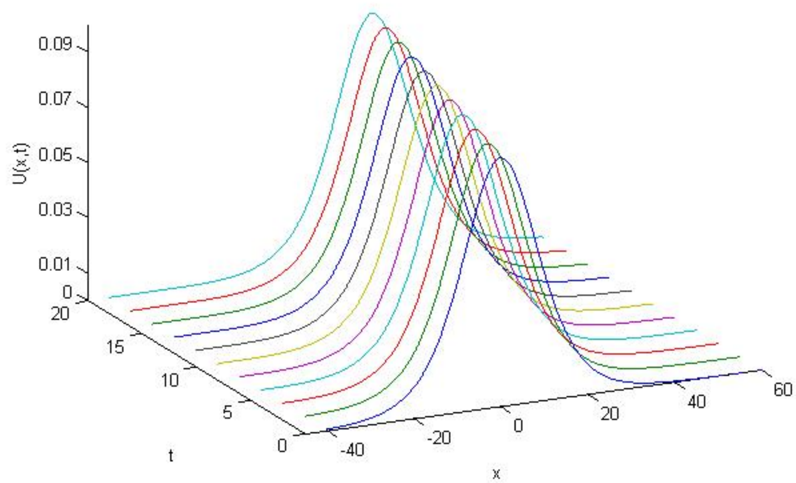

Figure 1: The single solitary wave with $c = 0.03$.

The analytical invariants obtained from Eq. (8) are $I_1 = 3.979950$, $I_2 = 0.810462$ and $I_3 = 2.579007$ for $c = 0.1$. Table 4 shows invariants and error norms for $c = 0.1$, $x^* = 0$ and $h = k = 0.2$ through the interval $-40 \leq x \leq 60$. The invariants and error norms are given for times up to $t = 20$ in Table 4. The profile of the solitary wave from $t = 0$ to $t = 20$ are compared in Fig. 2. Table 5 gives a comparison of invariants obtained by the present method and the other methods [5, 8, 15, 20, 25] for $c = 0.1$ at $t = 20$.

Table 4: Invariants and error norms for the single solitary wave for $h = k = 0.2$, $-40 \leq x \leq 60$ and $c = 0.1$.

t	I_1	I_2	I_3	L_2	L_∞
0	3.979926	0.810462	2.579007		
2	3.979941	0.810462	2.579007	0.000234	0.000090
4	3.979951	0.810462	2.579007	0.000466	0.000182
6	3.979956	0.810462	2.579007	0.000696	0.000275
8	3.979965	0.810462	2.579007	0.000922	0.000366
10	3.979970	0.810462	2.579007	0.001146	0.000454
12	3.979974	0.810462	2.579007	0.001365	0.000538
14	3.979974	0.810462	2.579007	0.001580	0.000620
16	3.979972	0.810462	2.579006	0.001791	0.000698
18	3.979963	0.810462	2.579006	0.001997	0.000773
20	3.979942	0.810462	2.579006	0.002198	0.000844

Table 5: Comparison of invariants for $-40 \le x \le 60$, $c = 0.1$ at $t = 20$.

Method	I_1	I_2	I_3
Analytical	3.979950	0.810462	2.579007
Present Method $(h = k = 0.2)$	3.979942	0.810462	2.579006
[5] $(h = 0.125, k = 0.1)$	3.98203	0.810467	2.57302
[8] $(h = 3, k = 0.01)$	3.990464	0.823457	2.673990
[15] $(h = 0.125, k = 0.1)$	3.978035	0.8097240	2.576573
[20] $(h = k = 0.1)$	3.9799065	0.8104625	2.5790074
[25] $(h = k = 0.1)$	3.97989	0.81046	2.57900

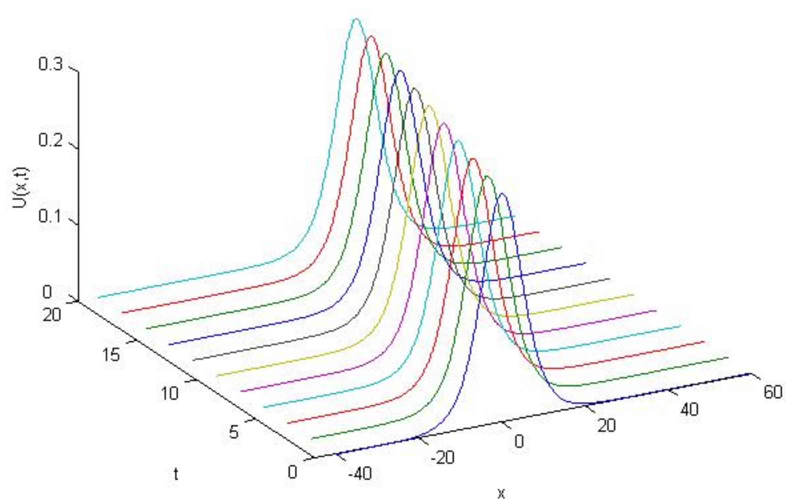

Figure 2: The single solitary wave with $c = 0.1$.

The analytical invariants for $c = 0.3$ obtained from Eq. (8) are $I_1 = 7.493998$, $I_2 = 4.703925$ and $I_3 = 16.726603$. Invariants and error norms are given in Table 6 for $c = 0.3$, $x^* = 40$, $h = 0.2$ and $k = 0.1$ through the interval $0 \le x \le 80$ for times up to $t = 10$. Fig. 3 indicates that the numerical solution of single solitary wave with $c = 0.3$ at different time. A comparison of invariants obtained by the present method and the results of reference[25] is given in Table 7 for $c = 0.3$ at $t = 10$.

Table 6: Invariants and error norms for the single solitary wave for $h = 0.2$, $k = 0.1$, $0 \leq x \leq 80$ and $c = 0.3$.

t	I_1	I_2	I_3	L_2	L_∞
0	7.493998	4.703923	16.726603		
1	7.493998	4.703924	16.726603	0.000925	0.000448
2	7.493997	4.703924	16.726601	0.001838	0.000911
3	7.493997	4.703924	16.726600	0.002732	0.001363
4	7.493997	4.703924	16.726598	0.003601	0.001790
5	7.493997	4.703924	16.726596	0.004442	0.002189
6	7.493996	4.703925	16.726593	0.005251	0.002555
7	7.493994	4.703925	16.726591	0.006028	0.002892
8	7.493991	4.703925	16.726589	0.006774	0.003204
9	7.493986	4.703925	16.726586	0.007490	0.003493
10	7.493976	4.703926	16.726584	0.008177	0.003771

Table 7: Comparison of invariants for $h = 0.2$, $k = 0.1$, $0 \leq x \leq 80$ and $c = 0.3$, at $t = 10$.

Method	I_1	I_2	I_3
Analytical	7.493998	4.703925	16.726603
Present Method	7.493976	4.703926	16.726584
[25]	7.493698	4.703578	16.725260

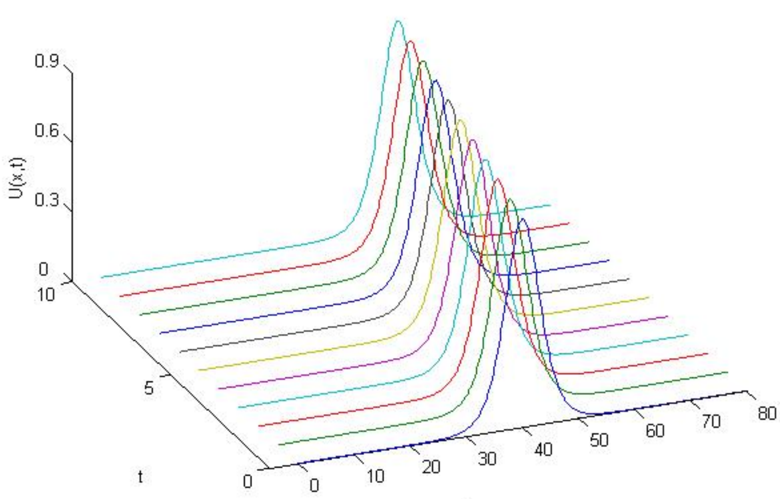

Figure 3: The single solitary wave with $c = 0.3$.

3.2 Interaction of Two Solitary Waves

Secondly, the interaction process of two solitary waves traveling in the same direction is studied using the initial condition

$$u(x,0) = 3c_1 \mathrm{sech}^2(p_1(x - x_1^*)) + 3c_2 \mathrm{sech}^2(p_2(x - x_2^*)) \tag{9}$$

where $c_j = 4p_j^2/\left(1 - 4p_j^2\right), j = 1, 2$ and the boundary condition $u \longrightarrow 0$ as $x \longrightarrow \pm\infty$. To allow comparison with the previous method, parameters are taken as $\mu = 1$ and $\varepsilon = 1$.

The analytical values of the invariant quantities are [25]

$$\begin{aligned} I_1 &= \frac{6c_1}{p_1} + \frac{6c_2}{p_2}, \\ I_2 &= \frac{12c_1^2}{p_1} + \frac{12c_2^2}{p_2} + \frac{48\mu}{5}\left(p_1c_1^2 + p_2c_2^2\right), \\ I_3 &= \frac{36c_1^2}{p_1}\left(1 + \frac{4c_1}{5}\right) + \frac{36c_2^2}{p_2}\left(1 + \frac{4c_2}{5}\right). \end{aligned} \tag{10}$$

Case I: In this case, to compare with earlier studies we take following parameters: $p_1 = 0.4$, $p_2 = 0.6$, $x_1^* = 23$ and $x_2^* = 38$ through the interval $0 \le x \le 80$. With these parameters, magnitude of the smaller solitary wave is 5.333333, magnitude of the larger solitary wave is -9.818182 and peak positions of them are located at $x_1^* = 23$ and $x_2^* = 38$. Table 8 displays numerical invariants for the interaction of two solitary waves for $h = 0.1$ and $k = 0.05$ with *Case I.* The analytical invariants obtained from Eq. (10) are $I_1 = -6.060606$, $I_2 = 382.859871$ and $I_3 = -350.928198$ for *Case I.* Comparison of invariants obtained from present method, analytical values and earlier method was developed by Raslan[25] is given in Table 9. Fig. 4 presents interaction of two solitary waves for *Case I* at $t = 0$ and $t = 10$.

Table 8: Invariants for the interaction of two solitary waves for Case I.

t	I_1	I_2	I_3
0	-6.060606	382.851454	-350.877818
1	-6.060606	382.849526	-350.864761
2	-6.060606	382.790118	-350.601913
3	-6.060606	381.807237	-349.257998
4	-6.060606	378.915497	-348.569184
5	-6.060606	378.151993	-348.861159
6	-6.060606	381.007422	-349.324782
7	-6.060605	382.193044	-350.452113
8	-6.060605	382.450093	-350.701980
9	-6.060605	382.554442	-350.632950
10	-6.060605	382.620734	-350.578870

Table 9: Comparison of invariants for Case I at $t = 10$.

Method	I_1	I_2	I_3
Analytical	-6.060606	382.859871	-350.928198
Present Method ($h = 0.1,\ k = 0.05$)	-6.060604	382.620734	-350.578870
[25] ($h = 0.1,\ k = 0.01$)	-6.046971	382.2275	-351.0175

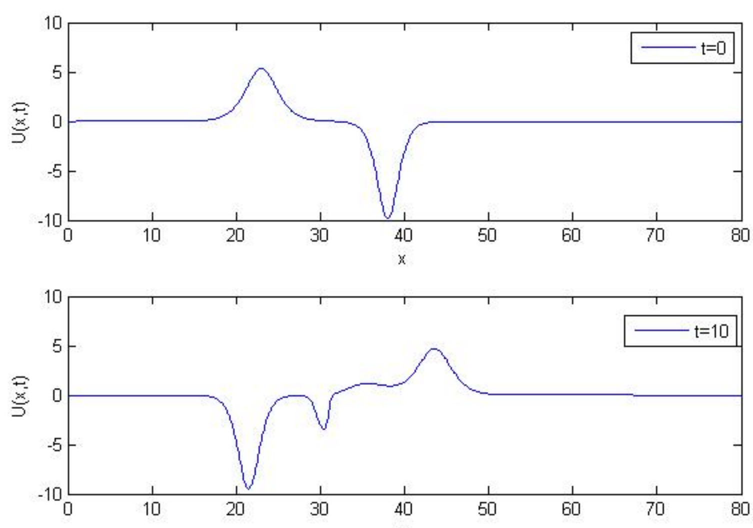

Figure 4: Interaction of two solitary waves for Case I.

Case II: In this case, parameters are $p_1 = 0.4$, $p_2 = 0.3$, $x_1^* = 15$ and $x_2^* = 35$ through the interval $0 \leq x \leq 120$. For *Case II*, the analytical invariants obtained from Eq. (10) are $I_1 = 37.916667$, $I_2 = 120.518611$ and $I_3 = 744.042342$. Numerical invariants for the interaction of two solitary waves for $h = 0.3$ and $k = 0.1$ with *Case II* are shown in Table 10. A comparison of invariants for this case is shown in Table 11. For *Case II*, magnitude of the larger solitary wave is 5.333333, magnitude of the smaller solitary wave is 1.687500 and peak positions of them are located at $x_1^* = 15$ and $x_2^* = 35$. As is well known, solitary waves with smaller amplitudes have a less velocity than another of larger amplitudes. It is shown from Fig. 5 that the larger wave catches up the smaller wave and passes it completely at $t = 25$.

Table 10: Invariants for the interaction of two solitary waves for Case II.

t	I_1	I_2	I_3
0	37.916482	120.520529	744.081209
2	37.916850	120.515270	743.998856
4	37.916972	120.513172	743.956686
6	37.917095	120.511737	743.917027
8	37.917203	120.507671	743.793804
10	37.917283	120.491639	743.320545
12	37.917338	120.454901	742.228425
14	37.917373	120.443678	741.553520
16	37.917398	120.482803	742.495915
18	37.917417	120.505286	743.432006
20	37.917435	120.509536	743.789261
22	37.917450	120.509401	743.886886
24	37.917461	120.508706	743.908045
25	37.917464	120.508347	743.909776

Table 11: Comparison of invariants for Case II at $t = 25$.

Method	I_1	I_2	I_3
Analytical	37.916667	120.518611	744.042342
Present Method ($h = 0.3, k = 0.1$)	37.917464	120.508347	743.909776
[8] ($h = 1, k = 0.1$)	38.050100	119.835500	727.439200
[20] ($h = 0.2, k = 0.1$)	37.91812	120.51241	744.00543
[25] ($h = 0.3, k = 0.1$)	37.91702	120.52249	744.07479

3.3 Interaction of Three Solitary Waves

Thirdly, the interaction process of two solitary waves traveling in the same direction is studied by using the initial condition

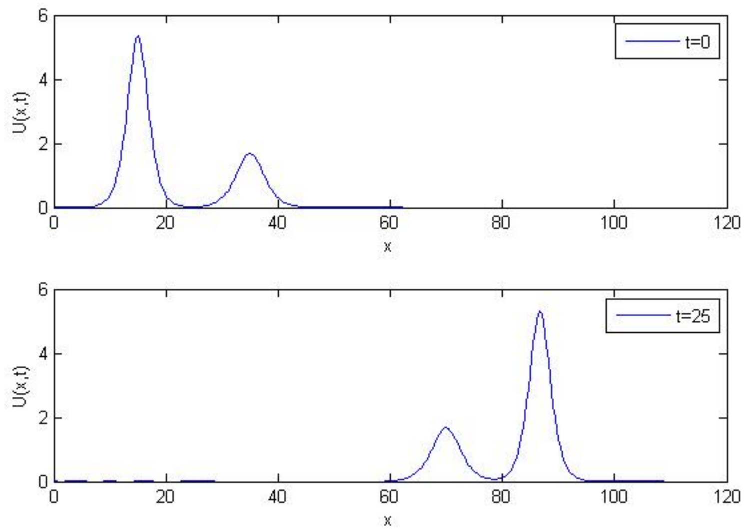

Figure 5: Interaction of two solitary waves for Case II.

$$\begin{aligned} u(x,0) &= 3c_1\mathrm{sech}^2(p_1(x-x_1^*))+3c_2\mathrm{sech}^2(p_2(x-x_2^*)) \\ &\quad +3c_3\mathrm{sech}^2(p_3(x-x_3^*)) \end{aligned} \tag{11}$$

where $p_j=\sqrt{c_j/4\mu\,(1+c_j)}$, $j=1,2,3$ and the boundary condition $u\longrightarrow 0$ as $x\longrightarrow\pm\infty$. To allow comparison with the previous method parameters are taken as $\mu=1$ and $\varepsilon=1$.

In this case, the following parameters are used: $c_1=0.6$, $c_2=0.3$, $c_3=0.15$, $x_1^*=15$, $x_2^*=35$ and $x_3^*=60$.

The analytical values of the invariant quantities are [25]

$$\begin{aligned} I_1 &= \frac{6c_1}{p_1}+\frac{6c_2}{p_2}+\frac{6c_3}{p_3}, \\ I_2 &= \frac{12c_1^2}{p_1}+\frac{12c_2^2}{p_2}+\frac{12c_3^2}{p_3}+\frac{48\mu}{5}\left(p_1c_1^2+p_2c_2^2+p_3c_3^2\right), \\ I_3 &= \frac{36c_1^2}{p_1}\left(1+\frac{4c_1}{5}\right)+\frac{36c_2^2}{p_2}\left(1+\frac{4c_2}{5}\right)+\frac{36c_3^2}{p_3}\left(1+\frac{4c_3}{5}\right). \end{aligned} \tag{12}$$

Thus $I_1=24.235523$, $I_2=21.405362$ and $I_3=84.394679$ are obtained from Eq. (12) for these parameters. In Table 12, we recorded invariants for the interaction of three solitary waves for $h=0.5$ and $k=0.25$ through the interval $0\leq x\leq 350$. It is shown from Fig. 6 that initial solitary waves have amplitudes $1.800242, 0.900250$ and 0.450022. Fig. 6 illustrates how the larger waves overtakes and passes through the smaller ones.

Table 12: Invariants for the interaction of three solitary waves.

t	I_1	I_2	I_3
0	24.234123	21.428863	84.504718
25	24.237740	21.428939	84.442842
50	24.237753	21.426899	84.265979
75	24.237876	21.429242	84.265328
100	24.237920	21.430516	84.427213
125	24.237378	21.430104	84.455941
150	24.237405	21.428956	84.462757
175	24.237574	21.427739	84.468773
200	24.133487	21.425923	84.455704

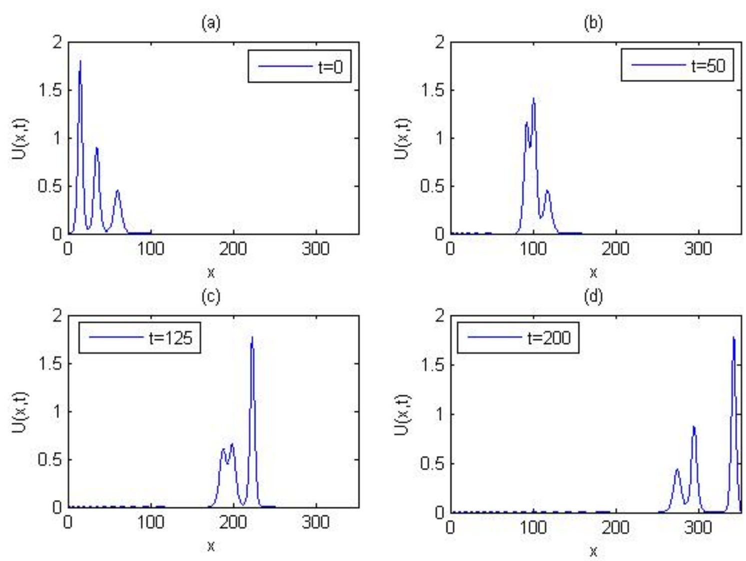

Figure 6: The three solitary waves at different times.

3.4 The Undular Bore

To model the development of an undular bore we use the initial condition given by

$$u(x,0) = \frac{u_0}{2}(1 - \tanh(\frac{x - x^*}{d})) \tag{13}$$

with the boundary conditions $u(a,t) = u_0$ and $u(b,t) = 0$. Under the boundary conditions the invariants I_1, I_2 and I_3 are not constant but increase linerarly throughout the simulation at the following rates [30]

$$\begin{aligned} M_1 &= \frac{dI_1}{dt} = u_0 + \frac{\varepsilon}{2} u_0^2, \\ M_2 &= \frac{dI_2}{dt} = u_0^2 + \frac{2\varepsilon}{3} u_0^3, \\ M_3 &= \frac{dI_3}{dt} = 3u_0^2 + (1+2\varepsilon)\, u_0^3 + \frac{3\varepsilon}{4} u_0^4. \end{aligned} \tag{14}$$

The theorical values for the growth rates in I_1, I_2 and I_3 are found $M_1 = 0.107500, M_2 = 0.011000$ and $M_3 = 0.034112$ from Eq. (14). To compare with the previous methods, parameters are taken as $\mu = \frac{1}{6}$, $\varepsilon = 1.5$, $u_0 = 0.1$, $x^* = 0$, $a = -36$, $b = 300$ and $d = 2$ and $d = 5$. The numerically growth rates in invariants can be computed from following equation [27].

$$M_j = \frac{I_j(t=800) - I_j(\ t=0)}{\text{time}},\ j = 1,2,3 \tag{15}$$

Table 13 displayed I_1, I_2 and I_3, the position and amplitude for $h = 2.4$, $k = 1.0$ and the gentle slope $d = 2$. The behavior of the wave with time for the gentle slope $d = 2$ is shown in Fig. 7.

Table 13: Invariants for the undular bore with $d = 2$.

t	I_1	I_2	I_3	x	U
0	3.480000	0.338156	1.047022		
50	8.854958	0.887423	2.752474	43.200000	0.133713
100	14.231579	1.437263	4.459113	96.000000	0.140891
150	19.605281	1.986525	6.163933	148.800000	0.148837
200	24.980616	2.536100	7.869790	201.600000	0.154721
250	30.355434	3.085564	9.575358	256.800000	0.158563

Table 14: Comparison of the growth rates in invariants for the undular bore with $d = 2$.

Method	M_1	M_2	M_3
Analytical	0.107500	0.011000	0.034112
Present Method ($h = 2.4,\ k = 1.0$)	0.107502	0.010990	0.034113
[13] ($h = 0.24,\ k = 0.1$)	0.1075	0.010999	0.034092
[19] ($h = 0.24,\ k = 0.1$)	0.107499	0.011	0.034095
[27] ($h = 0.24,\ k = 0.1$)	0.107500	0.010992	0.034096

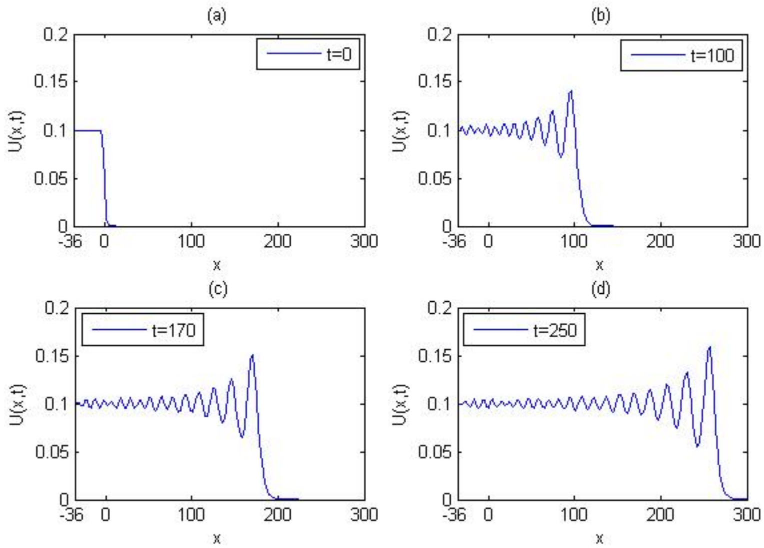

Figure 7: The undular bore with $d = 2$.

The invariants, the position and amplitude for $h = 2.4$, $k = 1.0$ and the gentle slope $d = 5$ recorded in Table 15. Fig. 8 shows the undular bore profiles at different time for $d = 5$. It can be seen clearly from both Fig. 7 and Fig. 8, the number of the produced waves increase when value of t increased. It is observed from Table 14 and Table 16 that the numerically growth rates in invariants is achieved to remain almost the same with analytical ones for the undular bore with the gentle slope $d = 2$ and $d = 5$.

Table 15: Invariants for the undular bore with $d = 5$.

t	I_1	I_2	I_3	x	U
0	3.480000	0.323110	1.000050		
50	8.855016	0.872790	2.705652	43.200000	0.120832
100	14.230100	1.422439	4.411334	96.000000	0.131956
150	19.604965	1.972000	6.116889	148.800000	0.142092
200	24.980024	2.521560	7.822574	201.600000	0.150291
250	30.354917	3.071068	9.528198	254.400000	0.153833

Table 16: Comparison of the growth rates in invariants for the undular bore with $d = 5$.

Method	M_1	M_2	M_3
Analytical	0.107500	0.011000	0.034112
Present Method ($h = 2.4, k = 1.0$)	0.107500	0.010992	0.034113
[13] ($h = 0.24,\ k = 0.1$)	0.1075	0.010999	0.034097
[19] ($h = 0.24,\ k = 0.1$)	0.107499	0.011	0.034099
[27] ($h = 0.24,\ k = 0.1$)	0.107500	0.010992	0.034101

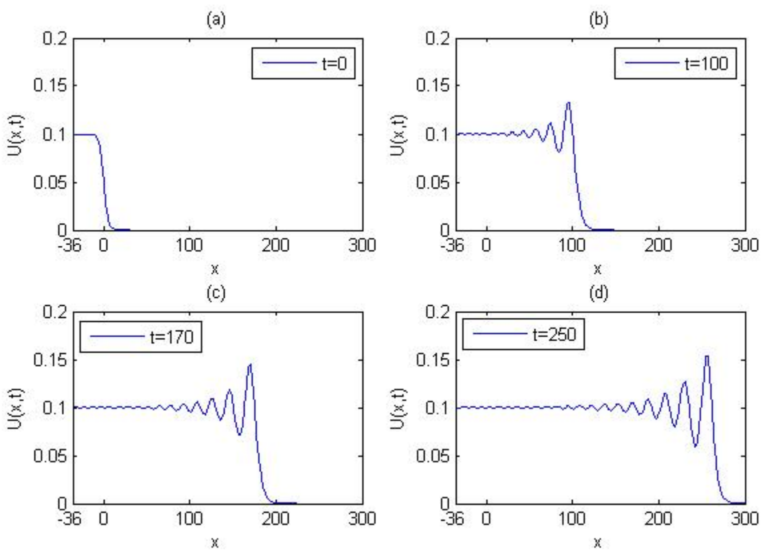

Figure 8: The undular bore with $d = 5$.

4 Conclusion

In this paper, a numerical solution algorithm for RLW equation has been considered using a fully implicit finite difference scheme. Numerical tests for single solitary wave, two solitary waves and interaction of three solitary waves are given. We also have examined two development of an undular bore. The numerical results demonstrate that the present method is quite accurate and readily implemented in the solution of the RLW equation. Thus, for the numerical solution of the RLW equation has defined an alternative method by this paper.

References

[1] A. Araújo and A. Durán, Error propagation in the numerical integration of solitary waves: The regularized long wave equation, *Appl. Num. Math.*, 36(2001), 197-217.

[2] A.R. Bahadır, Numerical solution for one-dimensional Burgers' equation using a fully implicit finite-difference method, *Int. J. Appl. Math.*, 1(1999), 897-909.

[3] A.R. Bahadır, A fully implicit finite-difference scheme for two-dimensional Burgers' equations, *Appl. Math. Comput.*, 137(2003), 131-137.

[4] D. Bhardwaj and R. Shankar, A computational method for regularized long wave equation, *Comput. Math. Appl.*, 40(2000), 1397-1404.

[5] İ. Dağ, Least-squares quadratic B-spline finite element method for the regularised long wave equation, *Comput. Methods Appl. Mech. Engrg.*, 182(2000), 205-215.

[6] İ. Dağ, A. Doğan and B. Saka, B- spline collocation methods for numerical solutions of the RLW equation, *Int. J. Comput. Math.*, 80(2003), 743-757.

[7] İ. Dağ, B. Saka and D. Irk, Galerkin method for the numerical solution of the RLW equation using quintic B-splines, *J. Comput. Appl. Math.*, 190(2006), 532-547.

[8] İ. Dağ, A. Korkmaz and B. Saka, Cosine expansion-based differential quadrature algorithm for numerical solution of the RLW equation, *Numer. Meth. Part. Differ. Equat.*, 26(2010), 544-560.

[9] A. Dogan, Numerical solution of regularized long wave equation using Petrov-Galerkin method, *Commun. Numer. Meth. Engrg.*, 17(2001), 485-494.

[10] A. Dogan, Numerical solution of RLW equation using linear finite elements within Galerkin's method, *Appl. Math. Model.*, 26(2002), 771-783.

[11] J.C. Elibeck and G.R. McGuire, Numerical study of the regularized long-wave equation I: Numerical methods, *J. Comput. Phys.*, 19(1975), 43-57.

[12] J.C. Elibeck and G.R. McGuire, Numerical study of the regularized long-wave equation II: Interaction of solitary waves, *J. Comput. Phys.*, 23(1977), 63-73.

[13] A. Esen and S. Kutluay, Application of a lumped Galerkin method to the regularized long wave equation, *Appl. Math. Comput.*, 174(2006), 833-845.

[14] L.R.T. Gardner and G.A. Gardner, Solitary waves of the regularized long-wave equation, *J. Comput. Phys.*, 91(1990), 441-459.

[15] L.R.T. Gardner, G.A. Gardner and A. Doğan, A least-squares finite element scheme for the RLW equation, *Commun. Numer. Meth. Engrg.*, 12(1996), 795-804.

[16] C.I. Gheorghiu, Stable spectral collocation solutions to a class of Benjamin Bona Mahony initial value problems, *Appl. Math. Comput.*, 273(2016), 1090-1099.

[17] B. İnan and A.R. Bahadır, A numerical solution of the equal width wave equation using a fully implicit finite difference method, *Turk. J. Math. Comput. Sci.*, Article ID 20140037(2014), 14 pages.

[18] P.C. Jain and L. Iskandar, Numerical solutions of the regularized long-wave equation, *Comput. Meth. Appl. Mech. Eng.*, 20(1979), 195-201.

[19] S. Kutluay and A. Esen, A finite difference solution of the regularized long-wave equation, *Math. Probl. Eng.*, (2006), 1-14.

[20] J. Lin, Z. Xie and J. Zhou, High-order compact difference scheme for the regularized long wave equation, *Commun. Num. Meth. Eng. Biomedical Appl.*, 23(2007), 135-156.

[21] B. Lin, Non-polynomial splines method for numerical solutions of the regularized long wave equation, *Int. J. Comput. Math.*, 92(2015), 1591-1607.

[22] P.J. Olver, Euler operators and conservation laws of the BBM equation, *Math. Proc. Cambridge Philos. Soc.*, 85(1979), 143-160.

[23] D.H. Peregrine, Calculations of development of an undular bore, *J. Fluid Mech.*, 25(1966), 321-330.

[24] J.I. Ramos, Solitary waves of the EW and RLW equations, *Chaos, Solitons and Fractals*, 34(2007), 1498-1518.

[25] K.R. Raslan, A computational method for the regularized long wave (RLW) equation, *Appl. Math. Comput.*, 167(2005), 1101-1118.

[26] B. Saka, İ. Dağ and A. Doğan, Galerkin method for the numerical solution of the RLW equation using quadratic B-splines, *Int. J. Comput. Math.*, 81(2004), 727-739.

[27] B. Saka and İ. Dağ, Quartic B-spline collocation algorithms for numerical solution of the RLW equation, *Numer. Meth. Part. Differ. Equat.*, 23(2007), 731-751.

[28] B. Saka, A. Şahin and İ. Dağ, B- spline collocation algorithms for numerical solutiojn of the RLW equation, *Numer. Meth. Part. Differ. Equat.*, 27(2011), 581-607.

[29] A.A. Soliman and K.R. Raslan, Collocation method using quadratic B-spline for the RLW equation, *Int. J. Comput. Math.*, 78(2001), 399-412.

[30] S.I. Zaki, Solitary wave of the splitted RLW equation, *Comput. Phys. Commun.*, 138(2001), 80-91.